# Molecular Thermodynamics for Protein Precipitation with a Polyelectrolyte

**Jianwen Jiang and John M. Prausnitz***

*Chemical Engineering Department, University of California, Berkeley, and Chemical Sciences Division, Lawrence Berkeley Laboratory, University of California, Berkeley, California 94720*

*Received: February 8, 1999*

A molecular−thermodynamic framework is developed for phase equilibria in an aqueous system containing a charged globular protein and an oppositely charged linear polyelectrolyte. The globular protein is represented by a spherical macroion with its coions; the linear polyelectrolyte is represented by a charged hard-sphere chain (polyion) with corresponding counterions. The potential of mean force contains Coulombic interactions between macroions, polyions, and small ions; long-range dispersion attractions between protein macroions; and hydrophobic macroion−polyion and macroion−macroion associations. Analytic expressions for thermodynamic properties are obtained, and liquid−liquid phase equilibria (precipitation) are calculated for model systems. Adding polyelectrolyte to a protein solution leads to precipitation, but further addition of polyelectrolyte leads to redissolution of the protein. This destabilization−restabilization phenomenon follows from electrostatic interactions with coupled polymer adsorption. The effects on phase equilibria of protein charge, protein size, association energy between protein−polyion, polyion chain length, and polyion charge density are investigated for model systems and compared with experimental data. Brief consideration is given to fractional precipitation for binary aqueous mixtures of proteins with different charge densities.

## 1. Introduction

Protein precipitation (liquid phase splitting) provides an effective method for raising the concentration of a protein in a dilute solution. Precipitation plays an important role in downstream processing in biotechnology.[1] A variety of precipitating agents can be used, varying from water-soluble low molecular weight liquids[2] to nonionic polymers[3] and polyelectrolytes (PE).[4,5] Use of an oppositely charged polyelectrolyte to precipitate a protein offers several advantages: high protein recoveries can be obtained with a small amount of PE while retaining the native state of a protein without loss of biological activity. The target protein can be recovered by adjusting pH or ionic strength after precipitation, and the PE may be recycled.

PEs are also used in other industrial applications,[6] such as water treatment, food processing, and manufacture of paints and colloidal suspensions. While interactions in colloidal dispersions are less complex than those in protein solutions, both have similar electrochemical properties; therefore, colloidal suspensions serve as models to test theoretical predictions for globular protein solutions.

Several experimental studies have been reported for protein precipitation using PEs. The most extensively studied proteins are lysozyme,[4,5] ovalbumin,[4] bovine serum albumin (BSA),[7] and catalase.[8] Oppositely charged polyelectrolytes include carboxymethyl cellulose (CMC),[4,9] polyacrylic acid (PAA),[6,8] and polymethacrylic acid (PMA).[7] CMC and PAA have been used to precipitate selectively proteins from an aqueous mixture on the basis of different affinities.[4,10] A comprehensive summary of these studies is given in a recent review.[11] Stabilization or destabilization of colloidal suspension by polyelectrolytes has also been reported, for example, for polystyrene latex or silica particles,[12−14] similar phase behavior was observed.

Experimental observations provide a general picture for protein or colloid precipitation by PEs. Precipitation is frequently interpreted as liquid−liquid phase separation rather than liquid−solid phase separation because the precipitated phase is osmotically swollen owing to retained counterions and with substantial hydration.[11] Evidence for such liquid−liquid equilibria has been reported for serum albumin with polydimethyldiallyl ammonium chloride (PDMDAAC),[15] and for precipitation of ionic surfactant with oppositely charged PE.[16,17] Initially, addition of PE to a colloidal or protein solution produces liquid−liquid phase separation (precipitation), denoting destabilization. Precipitation is enhanced with increased PE concentration. However, when increasing PE concentration beyond an optimal value, the precipitated protein (or aggregated colloid) redissolves, leading to restabilization. The concentration of PE required for destabilization or restabilization depends on the pH (corresponding to protein charge) of the protein solution or on the charge of the colloidal particle. Other factors such as ionic strength and molecular weight (MW) of PE play secondary roles.

Although protein precipitation and colloid flocculation with polyelectrolytes have been studied for many years, few theoretical studies have been directed toward understanding the mechanism of precipitation. The concept "polymer bridging" concerns particles joined by the same polymer chain; its efficiency is mainly related to MW of the polymer. This mechanism, originally proposed for nonionic polymer systems,[18] has been applied to PEs.[19] For those systems, however, it was recognized that the favorable electrostatic interactions between two oppositely charged solutes play a significant, perhaps overwhelming role. A combination of polymer bridging and electrostatic interactions has also been observed. For example, for precipitation of lysozyme by PAA[5] and polystyrene by cationic polymers,[20] polymer bridging is important at high MW of PE; in contrast, electrostatic interaction is important at low MW. Another prevailing mechanism is provided by the "charge-patch" (mosaic) concept[12,21] where attraction is attributed to

* To whom correspondence should be addressed.

10.1021/jp990455e CCC: $18.00 
Published on Web 06/11/1999

charge heterogeneity in a protein or colloidal particle, similar to attraction between dipoles. This mechanism provides a reasonable interpretation for those flocculation phenomena that could not be explained using polymer bridging or electrostatic interaction. In some cases, flocculation of colloidal suspensions by like-charged PE[22] or nonadsorbing PE[23] is due to a depletion force, causing particles to aggregate by exclusion of polymer molecules from the space between particles at small distances.

Based on electrostatic interactions, some models were proposed for protein or colloid precipitation.[24,25] However, in these phenomenological descriptions, both macroion and polyion are represented by random coils. With increasing applications of protein precipitation by PEs in bioengineering, a fundamental molecular description is desirable. Toward that end, perturbation theory has been applied for describing colloid[26] and protein[27,28] precipitation by nonionic polymers. Random-phase approximation (RPA) and integral-equation methods have been proposed to discuss protein precipitation by salt.[29,30]

This work considers liquid−liquid phase separation for a ternary solution (protein, polyelectrolyte, water). Our discussion is for a two-component system with water as a continuous medium. The interaction potentials between particles are estimated by continuum-averaged potential of mean force. All thermodynamic properties are expressed analytically. Attention is given to the effects of charge and size of protein, length and charge density of polyion, and association strength of hydrophobic interaction. Some results are also given for fractional separation of aqueous binary protein mixtures. Although the discussion presented here provides only a crude representation of protein−polyelectrolyte systems, that discussion identifies essential factors that determine protein or colloid precipitation by liquid phase splitting.

## 2. Interaction Potentials

In our two-component system, a globular protein particle with its coions is one component; a linear polyion with its counterions is the other component. The protein particle is represented by a macroion with number density $\rho_p$, diameter $\sigma_p$, and charge $Z_p e$ ($e$ is the charge of a proton); its coion is represented by a charged hard sphere with number density $\rho_1$, diameter $\sigma_1$, and valence $Z_1 = -1$. The polyion is represented by a freely tangent-joined, charged, hard-sphere chain with length $r$. A monomer (segment) in the chain may carry charge $Z_m = -1$ and diameter $\sigma_m$. The number density of monomers (in the chain) in solution is $\rho_m$. The polyion is electroneutralized by counterions carrying charge $Z_2 = 1$ with number density $\rho_2$ and diameter $\sigma_2$. The number density of polyion is $\rho_r = \rho_m/r$. Electroneutrality requires

$$\rho_p Z_p + \rho_1 Z_1 = 0 \tag{1.a}$$

$$\rho_m Z_m + \rho_2 Z_2 = 0 \tag{1.b}$$

All ions are embedded in a continuum with dielectric permittivity $\epsilon = \epsilon_0 \epsilon_r$ where $\epsilon_0$ is the vacuum permittivity and $\epsilon_r$ is the dielectric constant. Here, the polyion is modeled as a flexible chain where some, but not necessarily all, monomers are charged.

In our previous study of flexible linear polyelectrolyte solutions,[31,32] theoretical predictions for osmotic pressure are consistent with those from computer simulation and from experimental data. As shown in Figure 1, the polyion is a partially charged chain composed of $q$ repeated subchains, where $n^{(1)}$ and $n^{(2)}$ are, respectively, segment numbers of charged hard spheres and neutral hard spheres per subchain; chain length $r$ is given by:

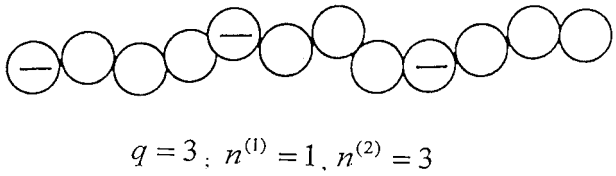


**Figure 1.** Schematic illustration of a partially charged polyion chain composed of $q$ repeated subchains. Here $n^{(1)}$ is the number of charged segments and $n^{(2)}$ is the number of neutral segments per subchain.

$$r = q(n^{(1)} + n^{(2)}) \tag{2}$$

We assume identical diameters for all segments in the polyion.

A molecular−thermodynamic description of protein or colloid precipitation requires an understanding of intermolecular forces in solution. Potential of mean force (PMF) serves to supply that understanding. Within the McMillan−Mayer framework, the PMF contains hard-sphere repulsions; electrostatic interactions between ions (including segments of polyion); dispersion interactions between protein particles; and protein−polyion and protein−protein associations.

Hard-sphere and Coulombic contributions are represented by

$$W_{ij}^{hs}(R) = \infty \quad R \le \sigma_{ij}$$
$$= 0 \quad R > \sigma_{ij} \tag{3}$$

$$W_{ij}^{ele}(R) = Z_i Z_j e^2/4\pi\epsilon R \tag{4}$$

where $R$ denotes the center-to-center distance and $\sigma_{ij} = (\sigma_{ij} + \sigma_j)/2$ is the additive diameter for $i$-$j$ interactions.

The attractive dispersion potential is proportional to $\sigma^6$, dominantly stronger for big particles than for small particles. Therefore, we only consider the dispersion potential between macroions, represented by[33]

$$W_{pp}^{dis}(R) = -H/36(\sigma_p/R)^6 \qquad R \ge \sigma_p \tag{5}$$

where $H$ is the Hamaker constant. Equation 5 gives a simplified long-range limit for the dispersion potential; it underestimates the contribution of the dispersion to the total PMF when $R$ approaches $\sigma_p$. However, because dispersion plays a minor role in our phase-equilibrium calculation, eq 5 is satisfactory for our purposes. Recent experimental work[34] indicates that $\beta H$ ($\beta = 1/kT$, $k$ is Boltzmann constant and $T$ is temperature) appears to be about 10. Therefore, in our calculations we consider $H$ a constant, independent of solution conditions.

There may be hydrophobic interaction between protein−polyion and protein−protein as a result of exposed nonpolar residues.[35] Hydrophobic bonds are formed when two hydrophobic groups come into contact with each other in aqueous solution leading to association. We use an association potential at contact to represent a hydrophobic interaction:

$$W_{ij}^{ass}(R) = -\xi_{ij} \quad R \in (\sigma_{ij} - w_{ij}, \sigma_{ij})$$
$$= 0 \qquad \text{otherwise} \tag{6}$$

where $w_{ij}$ is the association range. Experimental studies[36] show that the upper bound for the protein−protein association energy is $\beta\xi_{pp} = 5$. The association energy between protein and oppositely charged polyion $\beta\xi_{pr}$ is stronger than that for protein−protein. The number of association patches on protein and

polyion is $M_p$ and $M_r$ respectively. We assume that the association range $w$ is the same for all associations.

### 3. Thermodynamic Properties

The Helmholtz energy for our two-component system with total volume $V$ is obtained from perturbation theory for associated fluids:

$$\frac{\beta A}{V} = \frac{\beta A^{id}}{V} + \frac{\beta A^{hs}}{V} + \frac{\beta A^{ele}}{V} + \frac{\beta A^{dis}}{V} + \frac{\beta A^{chain}}{V} + \frac{\beta A^{ass}}{V} \quad (7)$$

The Helmholtz energy of the ideal gas mixture is given by[37]

$$\frac{\beta A^{id}}{V} = \sum_l \rho_l \ln(\rho_l \Lambda_l^3) - \sum_l \rho_l \quad (8)$$

where $\rho_l$ is the number density of molecules (not monomers) and $\Lambda_l$ denotes de Broglie wavelength. All other contributions are excess Helmholtz energies due to interactions.

Comparisons with Monte Carlo computer simulation[38] have shown that properties of hard-sphere mixtures can be reliably predicted from the BMCSL equation[39] even for a large diameter ratio. We therefore adopt that equation to account for the hard-sphere contribution from macroions, segments of polyions, counterions, and coions:

$$\frac{\beta A^{hs}}{V} = (\xi_2^3/\xi_3^2 - \xi_0)\ln\Delta + \frac{\pi\xi_1\xi_2/2 - \xi_2^3/\xi_3^2}{\Delta} + \frac{\xi_2^3/\xi_3^2}{\Delta^2} \quad (9)$$

where $\xi_n = \sum_k \rho_k \sigma_k^n$, $\Delta = 1 - \pi\xi_3/6$, and $\rho_k$ is the number density of particle $k$ where, for the polyion chain, $k$ refers to the monomer, i.e., before polyion chain formation.

For the contribution from electrostatic interactions, we use the mean spherical approximation (MSA)[40]

$$\frac{\beta A^{ele}}{V} = -\frac{\alpha_0^2}{4\pi}\left(\sum_k \frac{\rho_k Z_k^2 \Gamma}{1+\Gamma\sigma_k} + \frac{\pi P_n}{2\Delta}\sum_k \frac{\rho_k \sigma_k Z_k}{1+\Gamma\sigma_k}\right) + \frac{\Gamma^3}{3\pi} \quad (10)$$

where $\alpha_0^2 = \beta e^2/\epsilon$ is the Bjerrum length characterizing the dielectric property of the solvent and $\Gamma$ is the scaling parameter obtained from

$$4\Gamma^2 = \alpha_0^2 \sum_k \rho_k \left(\frac{1}{1+\Gamma\sigma_k}\right)^2 \left(Z_k - \frac{\pi P_n \sigma_k^2}{2\Delta}\right)^2 \quad (11)$$

$$P_n = \sum_k \frac{\rho_k \sigma_k Z_k}{1+\Gamma\sigma_k} \Big/ \left(1 + \frac{\pi}{2\Delta}\sum_k \frac{\rho_k \sigma_k^3}{1+\Gamma\sigma_k}\right) \quad (12)$$

An important advantage of the MSA is that thermodynamic properties can be obtained analytically, giving good agreement with experimental data.[41] The MSA has been widely used to study charged hard-sphere mixtures,[42] including those that are highly asymmetric,[43] and protein solutions.[27]

The contribution from dispersion attraction is obtained from the random phase approximation (RPA)[44] using the form previously presented for salting-out of proteins[29,30] and for asphaltene precipitation in crude oils:[45]

$$\frac{\beta A^{dis}}{V} = \frac{1}{2}\rho_p^2 U_{RPA} \quad (13)$$

where

$$U_{RPA} = \int_{\sigma_p}^{\infty} W_{pp}^{dis}(R)\, d\mathbf{R} = -\frac{\pi}{27}\beta H_p^3$$

The polyion is represented by a linear chain formed from charged hard-sphere segments. However, eqs 9 and 10 refer to monomers, not chain molecules. To correct for connectivity between chain segments, it is necessary to include a term $A^{chain}$ for the total Helmholtz energy. The Helmholtz energy attributed to chain formation has been given previously;[31,32] it is

$$\frac{\beta A^{chain}}{V} = \rho_r (1-r) \ln y_{mm}(\sigma_m) \quad (14)$$

Equation 14 is for a uniformly charged chain; it can be extended to a partially charged chain illustrated in Figure 1:

$$\frac{\beta A^{chain}}{V} = \rho_r [q(1-n^{(1)}) \ln y_{cc}(\sigma_c) + q(1-n^{(2)}) \ln y_{00}(\sigma_0) + (1-2q) \ln y_{c0}(\sigma_{c0})] \quad (15)$$

Here subscripts $c$ and 0, respectively, represent charged segment and neutral segment. The cavity correlation function at contact $y_{ij}(\sigma_{ij})$ is calculated from the hypernetted chain approximation (HNC) with the pair correlation function and the direct correlation function estimated from MSA[40]:

$$g_{ij}(\sigma_{ij}) = \frac{1}{\Delta} + \frac{\pi\sigma_i\sigma_j\xi_2}{4\Delta^2\sigma_{ij}} - \frac{\Gamma^2 a_i a_j}{\pi\sigma_{ij}\alpha_0^2} \quad (16)$$

$$c_{ij}(\sigma_{ij}) = -\frac{\alpha_0^2 Z_i Z_j}{4\pi\sigma_{ij}} \quad (17)$$

where parameter $a_i$ is given by

$$a_j = \frac{\alpha_0^2 (Z_i - \pi P_n \sigma_i^2/2\Delta)}{2\Gamma(1+\Gamma\sigma_i)} \quad (18)$$

In recent years, remarkable progress has been made toward a theory for associating fluids. The most successful statistical associated fluid theory (SAFT) originated from the seminal work of Wertheim[46] was developed by Chapman and co-workers.[47] Applying SAFT, the excess Helmholtz energy due to protein−protein and protein−polyion association is

$$\frac{\beta A^{ass}}{V} = M_p\rho_p\left(\ln x_p^a + \frac{1-x_p^a}{2}\right) + M_r\rho_r\left(\ln x_r^a + \frac{1-x_r^a}{2}\right) \quad (19)$$

where $x_p^a$ and $x_r^a$ are the fractions of sites not bonded on the surfaces of protein and polyion, respectively:

$$x_p^a = \frac{1}{1 + M_p\rho_p x_p^a \Delta_{pp} + M_r\rho_r x_r^a \Delta_{pr}} \quad (20.a)$$

$$x_r^a = \frac{1}{1 + M_p\rho_p x_p^a \Delta_{pr}} \quad (20.b)$$

with

$$\Delta_{pp} = g_{pp}(\sigma_p)[\exp(\beta\xi_{pp}) - 1]v_{pp}\sigma_p^3 \quad (21.a)$$

$$\Delta_{pr} = g_{pm}(\sigma_{pm})[\exp(\beta\xi_{pr}) - 1]v_{pm}\sigma_{pm}^3 \quad (21.b)$$

where $v_{ij}$ is a reduced volume corresponding to the volume of hydrophobic interaction between two sites *i*-*j*, related to square-well width *w*. We assume $v_{pp} = v_{pm} = v$ and that $g_{pm}(\sigma_{pm})$ is the pair correlation function at contact for protein and monomer of polyion given by eq 16. Similarly, $g_{pp}(\sigma_p)$ is that for two protein macroions, estimated by the EXP approximation[48]

$$g_{pp}(\sigma_p) = g_{pp}^{hs}(\sigma_p)\exp[-\beta W_{pp}^{ele}(\sigma_p) - \beta W_{pp}^{dis}(\sigma_p)] \quad (22)$$

Hydrophobic association between proteins is typically less than that between a protein and a polyion, i.e., $\xi_{pp} < \xi_{pr}$. Moreover, compared with $g_{pm}(\sigma_{pm})$, the value of $g_{pp}(\sigma_p)$ is small because of strong Coulombic repulsion between protein macroions; therefore, eq 20.a can be reasonably approximated by

$$x_p^a = \frac{1}{1 + M_r\rho_r x^a{}_r\Delta_{pr}} \quad (23)$$

Analytic solutions for $x_p^a$ and $x_r^a$ are

$$x_p^a = \frac{1}{2}\left[1 - \frac{1}{M_p\rho_p\Delta_{pr}} - \frac{M_r\rho_r}{M_p\rho_p} + \sqrt{\left(1 - \frac{1}{M_p\rho_p\Delta_{pr}} - \frac{M_r\rho_r}{M_p\rho_p}\right)^2 + \frac{4}{M_p\rho_p\Delta_{pr}}}\right] \quad (24.a)$$

$$x_r^a = \frac{1}{2}\left[1 - \frac{1}{M_r\rho_r\Delta_{pr}} - \frac{M_p\rho_p}{M_r\rho_r} + \sqrt{\left(1 - \frac{1}{M_r\rho_r\Delta_{pr}} - \frac{M_p\rho_p}{M_r\rho_r}\right)^2 + \frac{4}{M_r\rho_r\Delta_{pr}}}\right] \quad (24.b)$$

The osmotic pressure for our system is derived from

$$P = -\left[\frac{\partial A}{\partial V}\right]_{T,N} \quad (25)$$

where *N* is total particle number in the system. Combining with eq 7, we have the osmotic pressure as the sum of six contributions

$$P = P^{id} + P^{hs} + P^{ele} + P^{dis} + P^{chain} + P^{ass} \quad (26)$$

Appendix A gives analytic expressions for these contributions.

The chemical potential for each ion is obtained from

$$\mu_l = \left[\frac{\partial(A/V)}{\partial\rho_l}\right]_{T,V,N_{k\neq l}} \quad (27)$$

$$\mu_l = \mu_l^{id} + \mu_l^{hs} + \mu_l^{ele} + \mu_l^{dis} + \mu_l^{chain} + \mu_l^{ass} \quad (28)$$

where *l* represents protein macroion or polyion, or corresponding coion or counterion. Explicit expressions are outlined in Appendix B.

Precipitation of a protein (or a colloid) with a polyelectrolyte is here considered as liquid−liquid phase separation. At phase equilibrium, the concentrations of the two components in the precipitated phase and in the supernatant phase are calculated from the classical equilibrium conditions

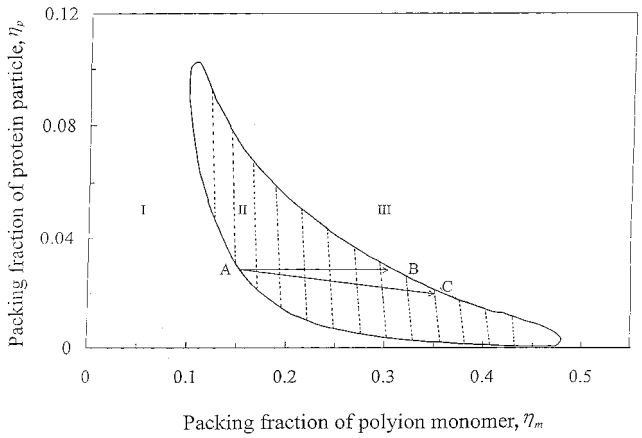


**Figure 2.** Phase diagram for a protein−polyelectrolyte system. Protein $Z_p = 3$; $\sigma_p = 30$ Å; polyion chain length $r = 1000$; $\beta\xi_{pr} = 10$. Here, I and III show one-phase regions; II shows a two-phase region. Nearly vertical dashed lines are tie lines. When polyelectrolyte is added to a solution at point A at constant volume, the two-phase region persists until B. However, when the accompanying change of volume is taken into account, the two-phase region persists until C.

$$P' = P'' \quad (29.a)$$

$$\mu'_{PR} = \mu''_{PR} \quad (29.b)$$

$$\mu'_{PE} = \mu''_{PE} \quad (29.c)$$

where prime and double prime designate equilibrated phases. Chemical potentials of the electrically neutral components protein (PR) and polyelectrolyte (PE) are given by

$$\mu_{PR} = (\rho_p\mu_p + \rho_1\mu_1)/(\rho_p + \rho_1) \quad (30.a)$$

$$\mu_{PE} = (\rho_r\mu_r + \rho_2\mu_2)/(\rho_r + \rho_2) \quad (30.b)$$

Equations (30.a) and (30.b) are equivalent to the standard definition of the chemical potential for an electrically neutral salt using stoichiometric coefficients.

## 4. Results and Discussion

In all calculations for liquid−liquid phase separations we set $T = 298.15$ K and dielectric constant $\epsilon_r = 78.3$, corresponding to an aqueous solution at room temperature. Sizes of monomer of polyion, coion 1, and counterion 2 are kept constant: $\sigma_m = 4.2$ Å; $\sigma_1 = 3.6$ Å; $\sigma_2 = 3.0$ Å. We set the number of association sites on a protein $M_p = 8$; for a polyion chain this number is much less than the number of chain segments (chain length) because of the steric hindrance of associated protein macroion, and we set $M_r = r/10$; the reduced association volume $v = 0.01$. We find that long-range dispersion interaction and hydrophobic protein−protein association play negligible roles. Without loss of generality, we assume $\beta H = 10$, $\beta\xi_{pp} = 2$.

Direct comparison with experiment is not possible because there are so many complicating factors in a real experiment.[7] Therefore, we present our calculations for model systems but, as shown later, we find semiquantitative agreement with experiment.

Figure 2 shows a liquid−liquid phase diagram for an aqueous protein−polyelectrolyte (PE) system with $Z_p = 3$, $\sigma_p = 30$ Å,

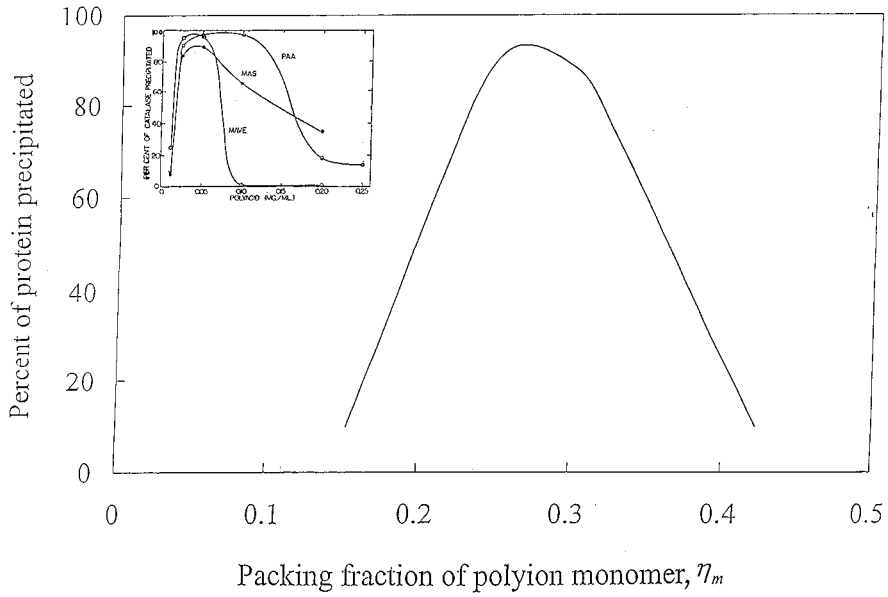


**Figure 3.** Effect of polyelectrolyte concentration on extent of protein precipitation. The insert shows experimental results for catalase precipitated by three polyacids: polyacrylic acid (PAA); maleic anhydride-styrene (MAS); maleic anhydride-vinyl methyl ether (MAVE) (ref 8).

$r = 1000$, and $\beta\xi_{pr} = 10$; here

$$\eta_p = \frac{\pi}{6}\rho_p\sigma_p^3$$

is the packing fraction of protein particles and

$$\eta_m = \frac{\pi}{6}\rho_m\sigma_m^3$$

is the packing fraction of polyion monomers. Areas I and III show one-phase regions; area II shows a two-phase region along with dashed tie lines. The upper curve represents the precipitated phase, the lower the supernatant phase. In the region where phase separation occurs, the concentration (number density) of protein is very dilute upon comparison with that of polyion monomer. The system is such that the protein particles are in a sea of polyion monomer. Thus, at phase separation, the concentrations of polyion monomer in the two phases are close to those before phase separation. At any given concentration in the two-phase region, phase separation occurs; the amount of two phases at equilibrium can be determined from the lever rule. The solubility of protein in a polyelectrolyte solution decreases with rising polyelectrolyte concentration, as observed in experiements.[7,9]

Figure 2 indicates the destabilization−restabilization phenomenon that has often been reported in experimental studies for protein or colloid systems. When PE is added to a protein solution, protein precipitates at a certain concentration of PE, for example, point A, the so-called critical precipitation concentration (CPC) where phase separation starts. In region II, additional PE leads to more precipitation. However, further increase of PE concentration beyond, for example, point B, leads to one phase again. Point B denotes restablization concentration (RSC).

Because this study is based on the McMillan−Mayer framework, solvent is not explicitly taken into account and therefore, according to McMillan−Mayer theory, destabilization (point A) and restabilization (point B) occur at constant concentration of protein, not consistent with practical studies where protein concentration decreases with addition of PE as a result of dilution. In practice, RSC will be at some arbitrary point C, chosen here for illustration only.

Figure 3 shows a schematic illustration of protein precipitated corresponding to path AC in Figure 2. Consistent with destabilization−restabilization, the amount of precipitated protein increases when PE is added, reaching a maximum as observed in practice. However, the amount of precipitation decreases with further addition of PE. Evidence for this phase behavior can be found in the experimental literature. The insert provides an example: catalase precipitated by one of three polyacids: polyacrylic acid (PAA), maleic anhydride-styrene (MAS), or maleic anhydride-vinyl methyl ether (MAVE).[8] Similar behavior was also observed in turbidimetric titration of bovine serum albumin (BSA) with polydimethyldiallyl ammonium chloride (PDMDAAC).[15,49]

Figure 4 shows the effect of protein macroion charge $Z_p$ on phase separation. Lower solubility in the supernatant phase is found upon decreasing $Z_p$. We expect that protein solubility reaches a minimum when the solution approaches its isoelectric point where the protein charge is close to zero, as experimentally observed.[7] The lower the protein charge, the lower are CPC and RSC. With decreased protein charge, less oppositely charged PE is needed to neutralize the protein, leading to protein precipitation. Also, less PE is required to reverse the charge on the protein−polyion complex, leading to restabilization. The effect of protein charge may also be observed if we change the pH of the protein solution because the protein charge varies with pH. The insert in Figure 4 shows percent of lysozyme removal by carboxymethyl cellulose (CMC) at various pH.[4] For lysozyme (isoelectric point IEP = 10.7[50]), the charges on protein at pH = 4.2, 5.8, 7.5 are 11, 7.5, 5.8, respectively.[51] As shown, a lower concentration of CMC is required to precipitate protein with smaller charge (higher pH). Similar behavior was also found for colloidal silica suspension with polyethyleneimine (PEI).[14]

Figure 5 shows the effect of protein macroion diameter $\sigma_p$ on protein precipitation. When protein size is reduced, more PE is required to precipitate protein and to restabilize protein as a result of the increase of protein charge density. The effect of protein diameter is more pronounced than that of protein

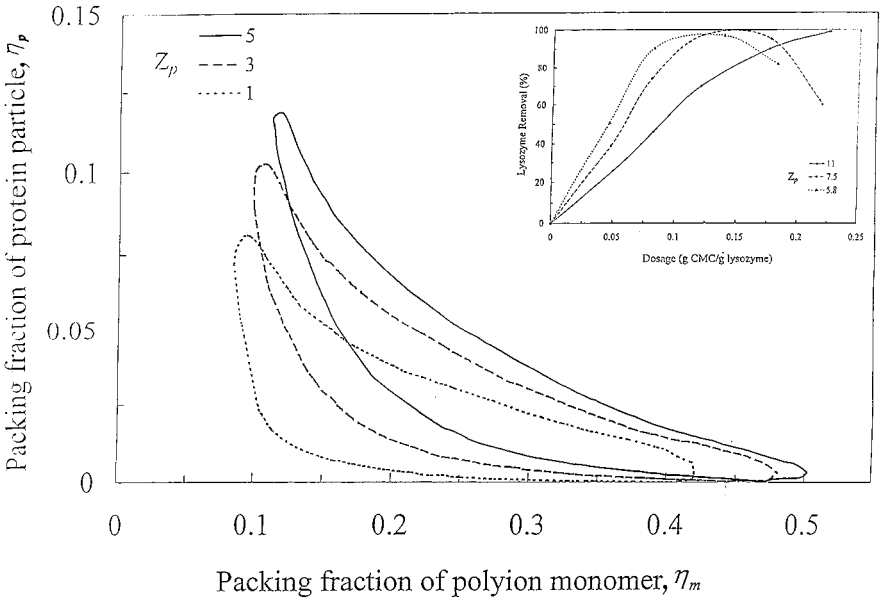


**Figure 4.** Effect of protein charge $Z_p$ on the phase diagram. Protein $\sigma_p = 30$ Å; polyion chain length $r = 1000$. The insert shows experimental results for the recovery of lysozyme by carboxymethyl cellulose (CMC) at various pH (ref 4).

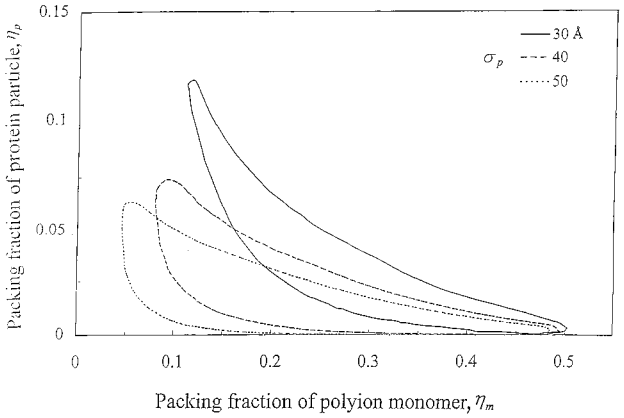


**Figure 5.** Effect of protein size $\sigma_p$ on the phase diagram. Protein $Z_p = 5$; polyion chain length $r = 1000$.

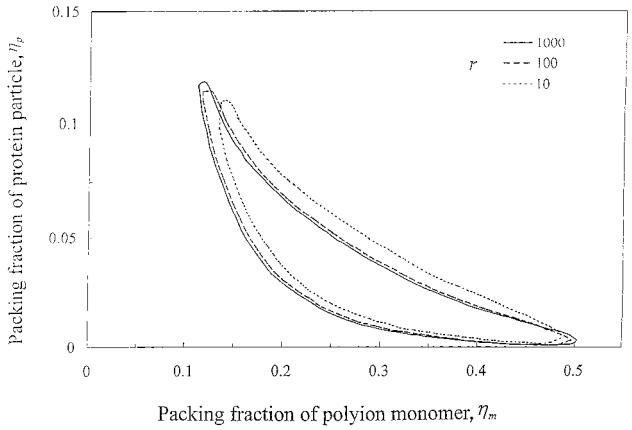


**Figure 6.** Effect of polyion chain length $r$ on the phase diagram. Protein $Z_p = 5$; $\sigma_p = 30$ Å.

charge because surface charge density is more sensitive to diameter according to $Z_p/\pi\sigma_p^2$.

We also examine the effect of association strength due to hydrophobic interaction between protein and polyion. The phase diagrams are almost the same at different association energies, indicating that, for the cases considered here, electrostatic interaction is more important than hydrophobic association.

Figure 6 shows the dependence of protein precipitation on polyion chain length $r$. When $r > 1000$, the phase diagrams are the same as that for $r = 1000$. However, when chain length shortens, both CPC and RSC rise slightly; the shorter $r$, the higher CPC and RSC. This effect cannot be accounted for by electrostatic interaction alone, but follows from electrostatic interaction with simultaneous polymer adsorption. Initially, polymer bridging causes precipitation. However, as PE concentration increases, formation of a steric layer favors restabilization. It is well known that a polymer with a shorter chain is less efficient for both bridging and steric restabilization.[52] As polymer length declines, more polymer is required as shown in our calculations and by experimental studies for lysozyme with polyacrylic acid (PAA)[5] and for colloidal silica suspension with polyethyleneimine (PEI).[13] The probable mechanism is schematically illustrated in Figure 7 where regions I, II, and III correspond to the three regions in Figure 2. With intermediate

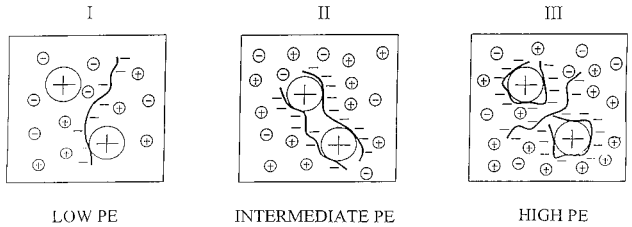


**Figure 7.** Schematic illustration of precipitation mechanism. Big spheres are protein macroions; dark lines are polyions. Small spheres (−) are coions of protein; small spheres (+) are counterions of polyion.

PE concentration, region II shows formation of bridging between particles, leading to precipitation. Upon increasing PE concentration, region III shows a steric layer surrounding the protein particle, leading to restabilization.

Polymer adsorption is mainly electrostatic induced; for the cases considered here, it is not due to hydrophobic association. Experimental studies[12] indicate an increase of the precipitation zone (two-phase region) with increasing molecular weight of polymer. The CPC decreases with molecular weight of polymer; in contrast, the RSC increases. This phenomenon is usually interpreted by charge patch model attributed to uneven charge distribution on the particles. However, this trend is not observed

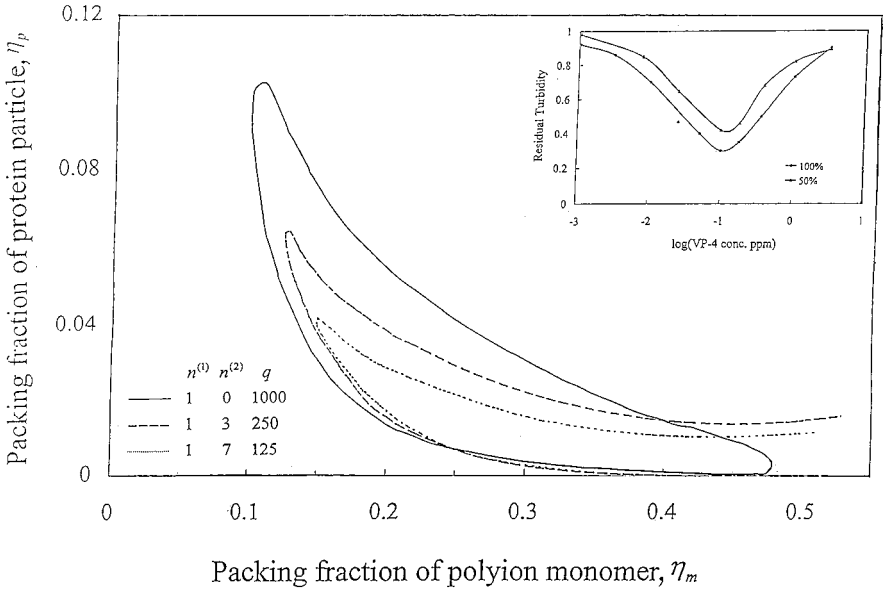


**Figure 8.** Effect of charge density of polyion chain on the phase diagram. Protein $Z_p = 3$; $\sigma_p = 30$ Å; $r = 1000$. The insert shows experimental residual turbidity for silica suspension flocculated by poly(*N*-methyl-4-vinylpyridinium iodide) (VP-4) at different surface charge densities (ref 14).

in our calculations because our description cannot account for nonuniform distribution of charged patches on the protein particles.

A more realistic polyelectrolyte is a copolymer where only a fraction of the monomers is charged, here represented by a partially charged hard-sphere chain. The effect of polyion charge density is shown in Figure 8 with constant chain length $r = 1000$. In the intermediate region, increased PE charge density produces a wider precipitation zone, i.e., a PE with higher charge density initiates the precipitation at lower concentration (CPC) and delays the restabilization at higher concentration (RSC). Evidence for this is shown in the insert for residual turbidity of silica suspension flocculated by poly(*N*-methyl-4-vinylpyridinium iodide) (VP-4) at different charge densities,[14] where low residual turbidity indicates flocculation. With increasing polyion charge density, the lower CPC is attributed to enhanced electrostatic interaction between PE and protein. However, high polyion charge density is unfavorable for the formation of a coupled steric layer as shown in Figure 7, because of the rigid configuration of PE, as suggested by several experimental studies[13,53] and by recent computer simulation.[54] At high PE concentration, it is likely that solid−liquid phase separation occurs, as indicated by studies of protein precipitation with nonionic polymer.[26−28]

Finally, we consider liquid−liquid phase separation for an aqueous mixture of two proteins A and B with same size 30 Å but different charge $Z_p^A = 6$, $Z_p^B = 1$, shown in Figure 9. Here $X_p^A$ and $X_p^B$ are mole fractions of two proteins on a water-free basis. Fractional precipitation is obtained with more protein B in the precipitated phase. We didn't perform calculations at a lower or higher PE concentration region where fractionation is small or even no fractionation (one phase); instead, more attention was given in the intermediate concentration region of PE where fractionation is more pronounced, similar to the case where we have only one protein.

With increased charge on protein *A* and $Z_p^A = 8$ and all other parameters unchanged, the phase diagram resembles that in Figure 10. The ratio of surface charge density $Z_p/\pi\sigma_p^2$ for proteins A to B (equal to 8) is now greater than that in Figure 9 (equal to 6). The minimum of $X_p^{B'}$ in the supernatant phase in Figure 9 approximates 0.28, but in Figure 10 it is 0.21; on the other hand, the corresponding $X_p^{B''}$ in the precipitated phase is nearly the same (= 0.75): from this we may say that the fractional precipitation (= $X_p^{B''}/X_p^{B'}$) is enhanced in Figure 10.

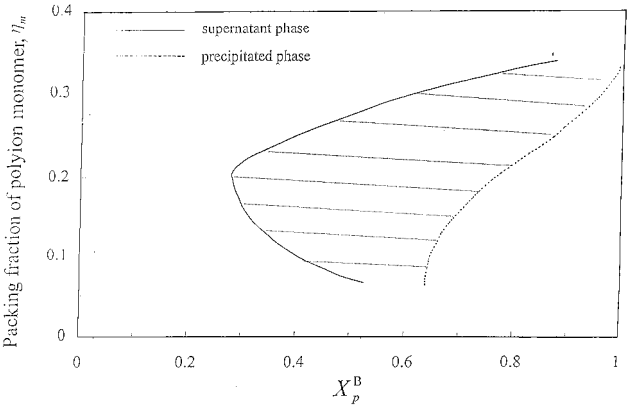


**Figure 9.** Effect of polyelectrolyte concentration on the phase diagram of an aqueous mixture containing two proteins with same size 30 Å but different charges $Z_p^A = 6$; $Z_p^B = 1$. Polyion chain length $r = 1000$. $X_p^B$ is mole fraction of protein B (water-free basis).

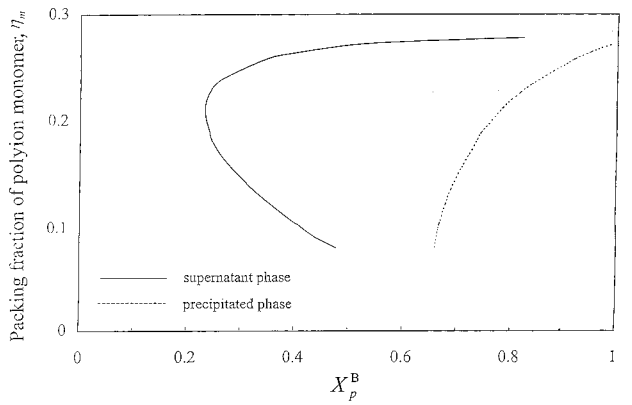


**Figure 10.** Effect of polyelectrolyte concentration on the phase diagram of an aqueous mixture containing two proteins with same size 30 Å but different charges $Z_p^A = 8$; $Z_p^B = 1$. Polyion chain length $r = 1000$. $X_p^B$ is mole fraction of protein B (water-free basis).

Finally, Figure 11 presents phase separation for an aqueous mixture of two proteins A and B with $Z_p^A = 6$, $\sigma_p^A = 30$ Å; $Z_p^B$

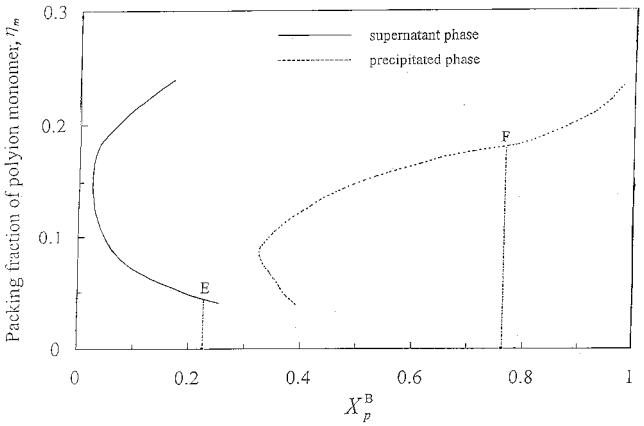


**Figure 11.** Effect of polyelectrolyte concentration on the phase diagram of an aqueous mixture containing two proteins with different charges and sizes: $Z_p^A = 6$; $\sigma_p^A = 30$ Å; $Z_p^B = 1$; $\sigma_p^B = 40$ Å. Polyion chain length $r = 1000$. Point E corresponds to experimental condition in ref 4 where the concentrations of both lysozyme and ovalbumin are 1 mg/mL. Point F corresponds to the condition where the concentrations of lysozyme and ovalbumin are 1 mg/mL and 10 mg/mL, respectively. $X_p^B$ is mole fraction of protein B (water-free basis).

$= 1$, $\sigma_p^B = 40$ Å. Much more fractional precipitation is obtained relative to those shown in Figures 9 and 10 because of a much larger surface charge density ratio of proteins A to B (equal to 10.7). Clark and Glatz[4] examined binary aqueous mixtures of lysozyme and ovalbumin precipitated by CMC. At pH = 4.2, the charge and size of lysozyme (protein A) are 11 and 30.4 Å; for ovalbumin (protein B) the charge is 6 and the size is 50 Å. In the experiment, the concentrations of both lysozyme (MW $= 1.3 \times 10^4$) and ovalbumin (MW $= 4.7 \times 10^4$) are 1 mg/mL, corresponding to point E in Figure 11. Upon increase of PE concentration at point E, initially the corresponding precipitated phase is $X^{B''}_p = 0.39$; this implies that at first mainly protein A (lysozyme) is precipitated. Upon further increase of PE concentration, $X^{B''}_p$ increases; that is, protein B (ovalbumin) co-precipitates. As observed experimentally, the protein A (lysozyme) with higher charge is selectively precipitated. However, we expect that, if concentrations of lysozyme and ovalbumin were 1 mg/mL and 10 mg/mL respectively, the system corresponds to point F. Upon increasing PE at point F, $X^{B''}_p$ in the precipitated phase is close to 0.8, indicating that the precipitated phase would be mainly composed of protein B (ovalbumin), suggesting that in this case, protein B with the lower charge is precipitated first.

## 5. Conclusion

For liquid−liquid precipitation of a protein by an oppositely charged polyelectrolyte, our calculations show that, upon increasing the concentration of PE, initially the system is in a one-phase region, then changes to a two-phase region, and finally recovers one phase, as experimentally observed. We have investigated the effects of protein charge and diameter, hydrophobic protein−polyion association, polyion chain length, and polyion surface charge density. Electrostatic interaction plays a dominant role, accompanied with coupled polymer adsorption as induced by electrostatic interaction but not by hydrophobic interaction. Our calculations confirm that the surface charge density of the protein particle is a dominant factor for protein precipitation. Secondary factors, polyion surface charge density and polyion molecular weight (chain length), play a minor role. We also obtained some results for aqueous binary mixtures of proteins with different charge densities giving fractional precipitation.

We recognize that precipitation in protein−polyelectrolyte systems is also influenced by other factors not considered here; at present, our understanding of these is far less mature. There are few general rules for any given system; usually we have to make a case-by-case study for a specific system. Nevertheless, the crude model developed here has probably captured most of the essential features of liquid−liquid precipitation in real protein−polyelectrolyte systems.

**Acknowledgment.** This work was supported by the Director, Office of Energy Research, Office of Basic Energy Sciences, Chemical Sciences Division of the U.S. Department of Energy, under Contract DE-AC03-76SF00098. The authors thank Prof. John Berg for providing the dissertation of Dr. Wen Chen and Prof. Herbert Morawetz for helpful advice. Additional support for J.W.J. by the Chinese National Science Foundation is acknowledged. J.W.J. is also grateful to Profs. Ying Hu and Honglai Liu (Shanghai) for their encouragement and to Dr. Jianzhong Wu and Van N. Nguyen for their kind help upon his arrival at the University of California, Berkeley.

## Appendix A. Osmotic Pressure

The osmotic pressure is

$$\beta P = \beta P^{id} + \beta P^{hs} + \beta P^{ele} + \beta P^{dis} + \beta P^{chain} + \beta P^{ass} \quad (A.1)$$

with

$$\beta P^{id} = \sum_l \rho_l \quad (A.2)$$

where $\rho_l$ is the number density of molecules (not monomers):

$$\beta P^{hs} = \frac{\pi\zeta_0\zeta_3}{6\Delta} + \frac{\pi\zeta_1\zeta_2}{2\Delta^2} + \frac{\pi^2(2+\Delta)\zeta_2^3}{36\Delta^3} \quad (A.3)$$

$$\beta P^{ele} = -\frac{\Gamma^3}{3\pi} - \frac{\alpha_0^2}{8}\left(\frac{P_n}{\Delta}\right)^2 \quad (A.4)$$

$$\beta P^{dis} = -\frac{\pi}{54}\beta H \rho_p^2 \sigma_p^3 \quad (A.5)$$

$$\beta P^{chain} = -\rho_r(r-1)\frac{\partial \ln y_{mm}(\sigma_m)}{\partial \ln \zeta_0} \quad (A.6)$$

The derivative of $y_{mm}(\sigma_m)$ with respect to density has been analytically derived previously.[31]

The association contribution to osmotic pressure $\beta P^{ass}$ can also be expressed analytically by combining eq 19 with eq 24.

## Appendix B. Chemical Potential

The chemical potential is

$$\beta\mu_l = \beta\mu_l^{id} + \beta\mu_l^{hs} + \beta\mu_l^{ele} + \beta\mu_l^{dis} + \beta\mu_l^{chain} + \beta\mu_l^{ass} \quad (B.1)$$

where subscript $l$ refers to protein macroion ($p$), polyion ($r$), coion (1), and counterion (2)

$$\beta\mu_l^{id} = \ln \rho_l \quad (B.2)$$

$$\beta\mu_l^{hs} = \begin{cases} r\beta\mu^{hs}{}_m & l = r \\ \beta\mu^{hs}{}_l & l = p, 1, 2 \end{cases} \quad (B.3)$$

where $m$ denotes monomer of polyion; $\beta\mu_k^{hs}$ ($k = m, p, 1, 2$) are

given by the BMCSL equation

$$\beta\mu_k^{\mathrm{hs}} = -\ln\Delta + \frac{\pi\sigma^3{}_k(\beta P^{\mathrm{hs}} + \zeta_0)}{6} + \frac{\pi\sigma_k(\sigma_k\zeta_1 + \zeta_2)}{2\Delta} + \frac{\pi^2\sigma_k^2\zeta_2^2}{8\Delta^2} + 3\left(\frac{\sigma_k\zeta_2}{\zeta_3}\right)^2\left(\ln\Delta + \frac{1-\Delta}{\Delta} - \frac{\pi^2\zeta_3^2}{72\Delta^2}\right) - \left(\frac{\sigma_k\zeta_2}{\zeta_3}\right)^3 \times \left(2\ln\Delta + \frac{(1-\Delta)(1+\Delta)}{\Delta}\right) \quad \text{(B.4)}$$

$$\beta\mu_l^{\mathrm{ele}} = \begin{cases} r\beta\mu^{\mathrm{ele}}{}_{\mathrm{m}} & l = r \\ \beta\mu^{\mathrm{ele}}{}_{l} & l = p, 1, 2 \end{cases} \quad \text{(B.5)}$$

where $\beta\mu_k^{\mathrm{ele}}$ ($k = m, p, 1, 2$) are derived from MSA

$$\beta\mu_k^{\mathrm{ele}} = \frac{2\Gamma a_k Z_k - \alpha_0^2 Z_k^2}{4\pi\sigma_k} - \frac{\sigma_k P_n(\Gamma a_k + \pi\alpha_0^2\sigma_k^2 P_n/12\Delta)}{4\Delta} \quad \text{(B.6)}$$

$$\beta\mu_l^{\mathrm{dis}} = \begin{cases} 0 & l = r, 1, 2 \\ -\dfrac{\pi}{27}\beta H\rho_{\mathrm{p}}\sigma_{\mathrm{p}}^3 & l = p \end{cases} \quad \text{(B.7)}$$

$$\beta\mu_l^{\mathrm{chain}} = \begin{cases} (1-r)\left[\ln y_{\mathrm{mm}}(\sigma_{\mathrm{m}}) + \rho_{\mathrm{m}}\dfrac{\partial \ln y_{\mathrm{mm}}(\sigma_{\mathrm{m}})}{\partial\rho_{\mathrm{m}}}\right] & l = r \\ (1-r)\rho_{\mathrm{r}}\dfrac{\partial \ln y_{\mathrm{mm}}(\sigma_{\mathrm{m}})}{\partial\rho_l} & l = p, 1, 2 \end{cases} \quad \text{(B.8)}$$

where

$$\frac{\partial \ln y_{\mathrm{mm}}(\sigma_{\mathrm{m}})}{\partial\rho_k}$$

($k = m, p, 1, 2$) are derived in a manner similar to that for

$$\frac{\partial \ln y_{\mathrm{mm}}(\sigma_{\mathrm{m}})}{\partial\zeta_0}$$

in eq A.6

$$\frac{\partial \ln y_{\mathrm{mm}}(\sigma_{\mathrm{m}})}{\partial\rho_k} = \frac{\pi\sigma_k^3}{6\Delta^2} + \frac{\pi\sigma_{\mathrm{m}}\sigma_k^2(\Delta + \pi\sigma_k\zeta_2/3)}{4\Delta^3} - \frac{2\Gamma a_{\mathrm{m}}}{\pi\alpha_0^2\sigma_{\mathrm{m}}}\left(a_{\mathrm{m}}\frac{\partial\Gamma}{\partial\rho_k} + \Gamma\frac{\partial a_{\mathrm{m}}}{\partial\rho_k}\right) \quad \text{(B.9)}$$

with

$$\frac{\partial\Gamma}{\partial\rho_k} = \frac{\alpha_0^2 Z_k^2/(1+\Gamma\sigma_k)^2}{8\Gamma + 2\alpha_0^2\sum_l \dfrac{\rho_l Z_l^2\sigma_l}{(1+\Gamma\sigma_l)^3}} \quad \text{(B.10)}$$

$$\frac{\partial a_{\mathrm{m}}}{\partial\rho_k} = -\frac{\alpha_0^2 Z_{\mathrm{m}}(1+2\Gamma\sigma_{\mathrm{m}})}{2\Gamma^2(1+\Gamma\sigma_{\mathrm{m}})^2}\cdot\frac{\partial\Gamma}{\partial\rho_k} \quad \text{(B.11)}$$

## References and Notes


(1) Scopes, R. K. *Protein Purification: Principles and Practices*, 3rd ed.; Springer-Verlag: New York, 1994.

(2) Shih, Y. C.; Prausnitz, J. M.; Blanch, H. W. *Biotech. Bioeng*. **1992**, *40*, 1155.

(3) Haire, R. N.; Tisel, W. A.; White, J. C.; Rosenberg, A. *Biopolymers* **1984**, *23*, 2761.

(4) Clark, K. M; Glatz, C. E. In *Downstream Processing and Bioseparation*; Hamel, J. F., Ed.; ACS Symposium Series 419; American Chemical Society: Washington, DC, 1990; Chapter 9 and references therein.

(5) Chen, W. *Protein precipitation by polyelectrolytes*, PhD Thesis; University of Washington, Seattle, 1992. Chen, W.; Walker, S.; Berg, J. C. *Chem. Eng. Sci*. **1992**, *47*, 1039. Chen, W.; Berg, J. C. *Chem. Eng. Sci*. **1993**, *48*, 1775.

(6) Attia, Y. A. *Flocculation in Biotechnology and Separation Systems*, Elsevier: New York, 1987.

(7) Morawetz, H; Hughes, W. L. *J. Phys. Chem*. **1952**, *56*, 64.

(8) Berdick, M.; Morawetz, H, *J. Biol. Chem*. **1953**, *206*, 959.

(9) Hidalgo, J; Hansen, P. M. T. *J. Agr. Food Chem*. **1969**, *17*, 1089.

(10) Sternberg, M.; Hershberger, D. *Biochim. Biophys. Acta* **1974**, *342*, 195.

(11) Dubin, P. L.; Gao, J.; Mattison, K. *Sep. Purif. Methods* **1994**, *23*, 1.

(12) Gregory, J. *J. Colloid Interf. Sci*., **1973**, *42*, 448; **1976**, *55*, 35.

(13) Lindquist, G. M.; Stratton R. A. *J. Colloid Interface Sci*. **1976**, *55*, 45.

(14) Bleier A.; Goddard, E. D. *Colloids Surf*. **1980**, *1*, 407.

(15) Dubin, P.; Ross, T. D.; Sharma, I.; Yegerlehner, B. In *Ordered Media in Chemical Separations*: Hinze, W. L, Armstrong D. W., Eds.; American Chemical Society: Washington, DC, 1987; Chapter 8.

(16) Lenk, T; Theis, C. In *Coulombic Interactions in Macromolecular Systems*; Eisenberg, A., Bailey, F. E., Eds.; American Chemical Society, Washington, DC, 1986; Chapter 20.

(17) Thalberg, K.; Lindman B.; Karlström, G. *J. Phys. Chem*. **1991**, *95*, 6004.

(18) Mer La, V. K.; Healy, T. W. *Rev. Pure Appl. Chem*. **1963**, *13*, 112.

(19) Herrington, T. M.; Midmore, B. R.; Watts, J. C. In *Colloid-Polymer Interactions: Particulate, Amphiphilic and Biological Surfaces*; Dubin, P., Tong P., Eds.; ACS Symposium Series 532; American Chemical Society: Washington, DC, 1993; Chapter 14.

(20) Gregory, J. *Trans. Faraday Soc*. **1969**, *65*, 2260.

(21) Kasper, D. R. *Theoretical and Experimental Investigations of the Flocculation of Charged Particles in Aqueous Solutions by Polyelectrolytes of Opposite Charge*; PhD Thesis; California Institute of Technology, Pasadena, 1971.

(22) Morvan, M.; Espinat, D.; Vason, R.; Lambard, J.; Zemb, Th. *Langmuir* **1994**, *10*, 2566.

(23) Cawdery, N.; Vincent B. In *Colloidal Polymer Particles*; Goodwin, J. W., Buscall, R., Eds.; Academic Press: New York, 1995; p 245. Nashima, T.; Sudo, H.; Furusawa, K. *Colloids Surf*. **1992**, *67*, 95.

(24) Veis, A.; Aranyi, C. *J. Phys. Chem*. **1960**, *64*, 1203. Tainiak, K. *J. Phys. Soc. Jpn*. **1990**, *46*, 1899.

(25) Clark, K. M.; Glatz, C. E. *Chem. Eng. Sci*. **1992**, *47*, 215.

(26) Gast A. P.; Hall, C. K.; Russel W. B. *J. Colloid Interface Sci*. **1983**, *96*, 251; *Faraday Discuss. Chem. Soc*. **1983**, *76*, 189.

(27) Mahadevan, H.; Hall, C. K. *AIChE J*. **1990**, *36*, 1517; **1992**, *38*, 573.

(28) Tavares, F. W.; Sandler, S. I. *AIChE J*. **1997**, *43*, 218.

(29) Vlachy V.; Blanch, H. W.; Prausnitz, J. M. *AIChE J*. **1993**, *39*, 215.

(30) Chiew, Y. C.; Kuehner D.; Blanch, H. W.; Prausnitz, J. M. *AIChE J*. **1995**, *41*, 2150.

(31) Jiang, J. W.; Liu, H. L.; Hu Y.; Prausnitz, J. M. *J. Chem. Phys*. **1998**, *108*, 780.

(32) Jiang, J. W.; Liu, H. L.; Hu Y. *J. Chem. Phys*. **1999**, *110*, 4952.

(33) Verwey, E. J. W; Overbeek, J. Th. G. *Theory of the Stability of Lyophobic Colloids*; Elsevier: New York, 1948.

(34) Coen, C. J.; Blanch, H. W.; Prausnitz, J. M. *AIChE J*. **1995**, *41*, 996.

(35) Sedlak, E.; Antalik M. *Biopolymers* **1998**, *46*, 145.

(36) Tanford, C. *The Hydrophobic Effect: Formation of Micelles and Biological Membranes*, 2nd ed.; Wiley: New York, 1980.

(37) Lee, L. L. *Molecular Thermodynamics of Nonideal Fluids*; Butterworth: Boston, 1988.

(38) Yau, D. L. H.; Chan, K. Y.; Henderson, D. *Mol. Phys*. **1996**, *88*, 1237.

(39) Boublik, T. *J. Chem. Phys*. **1990**, *53*, 471. Mansoori, G. A.; Carnahan, N. F.; Starling, K. E.; Leland, T. W. *J. Chem. Phys*. **1971**, *54*, 1523.

(40) Blum, L. *Mol. Phys*. **1975**, *30*, 1529. Blum L.; Hoye J. S. *J. Phys. Chem*. **1977**, *81*, 1311.

(41) Triolo, R.; Grigera, J. R.; Blum, L. *J. Phys. Chem*. **1976**, *77*, 1856. Vericat, F.; Grigera, J. R. *J. Phys. Chem*. **1982**, *86*, 1030.

(42) Kenkare, P. U.; Hall, C. K.; Caccamo, C. *J. Chem. Phys*. **1995**, *103*, 8098, 8111.

(43) Belloni, L. *J. Chem. Phys*. **1988**, *88*, 5143. Caccamo, C. *J. Chem. Phys.* **1989**, *91*, 4902.

(44) Evans, R.; Sluckin, T. J. *J. Phys. C* **1981**, *14*, 2569. Grimson, M. J. *J. Chem. Soc., Farad. Trans*. **1983**, *79*, 817.

(45) Wu J. Z.; Prausnitz, J. M.; Firoozabadi, A. *AIChE J*. **1998**, *44*, 1188.

(46) Wertheim, M. S. *J. Stat. Phys*. **1986**, *42*, 459, 477.

(47) Jackson G.; Chapman, W. G.; Gubbins, K. E. *Mol. Phys*. **1988**, *65*, 1. Chapman, W. G.; Jackson G.; Gubbins, K. E. *Mol. Phys.* **1988**, *65*, 1057.

(48) Konior, J.; Jedrzejek, C. *Mol. Phys.* **1985**, *55*, 187.

(49) Ahmed, L. S.; Xia, J. L. Dubin, P. L. *J. Macromol. Sci. Pure Appl. Chem.* **1994**, *31*, 17.

(50) Righetti, P.; Tudor, G.J. Chromatogr. 1981, 220, 115.

(51) Beychok, S.; Warner, R. C. *J. Am. Chem. Soc*. **1959**, *81*, 1892.

(52) Fleer, G. J.; Cohen Stuart, M. A.; Scheutjens, J. M. H. M.; Cosgrove, T.; Vincent B. *Polymers at Interfaces*; Chapman & Hall: London, 1993.

(53) Cosgrove, T.; Obey, T. M.; Vincent B. *J. Colloid Interface Sci*. **1986**, *111*, 409. Mabire, F.; Audebert, R.; Quivoron, C. *J. Colloid Interface Sci*. **1984**, *97*, 120.

(54) Wallin T.; Linse, P. *J. Chem. Phys*. **1998**, *109*, 5089.